Atmos. Chem. Phys. Discuss., 15, 33003–33048, 2015
www.atmos-chem-phys-discuss.net/15/33003/2015/
doi:10.5194/acpd-15-33003-2015

Atmospheric Chemistry and Physics Discussions

Analysis of the potential of near ground measurements of CO_2 and CH_4 in London, UK for the monitoring of city-scale emissions using an atmospheric transport model

A. Boon[1], G. Broquet[2], D. J. Clifford[1], F. Chevallier[2], D. M. Butterfield[3], I. Pison[2], M. Ramonet[2], J. D. Paris[2], and P. Ciais[2]

[1]Department of Meteorology, University of Reading, Reading, Berkshire RG6 6BB, UK
[2]Laboratoire des Sciences du Climat et de l'Environnement, CEA-CNRS-UVSQ, UMR8212, IPSL, Gif-sur-Yvette, France
[3]National Physical Laboratory, Teddington, Middlesex, TW11 0LW, UK

Received: 2 September 2015 – Accepted: 5 November 2015 – Published: 24 November 2015

Correspondence to: A. Boon (alex.boon@reading.ac.uk)

Published by Copernicus Publications on behalf of the European Geosciences Union.

Abstract

Carbon dioxide (CO_2) and methane (CH_4) mole fractions were measured at four near ground sites located in and around London during the summer of 2012 in view to investigate the potential of assimilating such measurements in an atmospheric inversion system for the monitoring of the CO_2 and CH_4 emissions in the London area. These data were analysed and compared with simulations using a modelling framework suited to building an inversion system: a 2 km horizontal resolution South of England configuration of the transport model CHIMERE driven by European Centre for Medium-Range Weather Forecasting (ECMWF) meteorological forcing, coupled to a 1 km horizontal resolution emission inventory (the UK National Atmospheric Emission Inventory). First comparisons reveal that local sources have a large impact on measurements and these local sources cannot be represented in the model at 2 km resolution. We evaluate methods to minimise some of the other critical sources of misfits between the observation data and the model simulation that overlap the signature of the errors in the emission inventory. These methods should make it easier to identify the corrections that should be applied to the inventory. Analysis is supported by observations from meteorological sites around the city and a three-week period of atmospheric mixing layer height estimations from lidar measurements. The difficulties of modelling the mixing layer depth and thus CO_2 and CH_4 concentrations during the night, morning and late afternoon led us to focus on the afternoon period for all further analyses. The misfits between observations and model simulations are high for both CO_2 and CH_4 (i.e., their root mean square (RMS) is between 8 and 12 parts per million (ppm) for CO_2 and between 30 and 55 parts per billion (ppb) for CH_4 at a given site). By analysing the gradients between the urban sites and a suburban or rural reference site, we are able to decrease the impact of uncertainties in the fluxes and transport outside the London area and in the model domain boundary conditions, and to better focus attention on the signature of London urban CO_2 and CH_4 emissions. This considerably improves the statistical agreement between the model and observations for CO_2 (model–data RMS

ACPD
15, 33003–33048, 2015

misfit of between 3 and 7 ppm) and to a lesser degree for CH_4 (model–data RMS misfit of between 29 and 38 ppb). Between one of the urban sites and either reference site, selecting the gradients during periods wherein the reference site is upwind of the urban site further decreases the statistics of the misfits in general even though not systematically. In a final attempt to focus on the signature of the city anthropogenic emission in the mole fraction measurements, we use a theoretical ratio of gradients of CO to gradients of CO_2 from fossil fuel emissions in the London area to diagnose observation based fossil fuel CO_2 gradients, and compare them with the modelled ones. This estimate increases the consistency between the model and the measurements when considering one of the urban sites, but not when considering the other. While this study evaluates different approaches for increasing the consistency between the mesoscale model and the near ground data, and manages to decrease the random component of the analysed model data misfits to an extent that should not be prohibitive to extracting the signal from the London urban emissions, large biases remain in the final misfits. These biases are likely to be due to local emissions, to which the urban near ground sites are highly sensitive. This questions our current ability to exploit urban near ground data for the atmospheric inversion of city emissions based on models at spatial resolution coarser than 2 km.

1 Introduction

As major emitters, cities have an important part to play in national greenhouse gas (GHG) emissions reporting. Over half of the world's population now live in cities and the UN estimate that the urban population will almost double from 3.4 to 6.3 billion by 2050 (United Nations, 2012). In the face of this continued urban population increase, cities can expect increased anthropogenic emissions unless measures are taken to reduce the impact of city life on the atmosphere. The majority of anthropogenic CO_2 is released in the combustion of fossil fuels for heating, electricity and transport, the latter of which is particularly important in the urban environment. The major sources

ACPD
15, 33003–33048, 2015

of CH_4 in city environments are leakage from natural gas infrastructure, landfill sites, wastewater treatment and transport emissions (Lowry et al., 2001; Nakagawa et al., 2005; Townsend-Small et al., 2012).

International agreements to limit GHG emissions make use of countries' self-reporting of emissions using emissions inventories. These inventories are based upon activity data and corresponding emissions factors and uncertainties can be substantial, particularly at city scale. Ciais et al. (2010a) showed uncertainties of 19 % of the mean emissions at country scale in the 25 EU Member States and up to 60 % at scales less than 200 km. Currently there is no legal obligation for individual cities to report their emissions; however, as environmental awareness increases and actions are taken to reduce urban emissions, monitoring of emissions to evaluate the success of emissions reduction schemes becomes an important consideration.

Quantifying GHG emissions from cities using atmospheric measurements is a relatively new scientific endeavour (Levin et al., 2011; McKain et al., 2012; Kort et al., 2013; Bréon et al., 2015). Determining the fluxes responsible for the measured GHG mole fractions requires the use of an atmospheric inversion scheme, typically by combining the measurements with an atmospheric transport model driven by a high resolution inventory (Levin et al., 2011). Instrumentation has been placed on tall masts or towers (> 50 m) or at near ground (sub-20 m) heights (Bréon et al., 2015; Lac et al., 2013; McKain et al., 2012) with a preference generally given to higher level measurement sites as these are expected to reduce variability due to local sources (Ciais et al., 2010b). In the UK, the central London 190 m British Telecom (BT) tower site was used by Rigby et al. (2008) and Helfter et al. (2011) in initial attempts to isolate London's CO_2 emissions. Rigby et al. (2008) compared CO_2 measurements from the BT tower site and near ground measurements at a more rural location upstream of the city in the prevailing wind direction. Helfter et al. (2011) used the eddy covariance technique to derive CO_2 local flux measurements and combined them together with an analytical footprint model to infer CO_2 emissions from specific London boroughs. The atmospheric inversion approach, assimilating the CO_2 measurements, has the potential to

ACPD
15, 33003–33048, 2015

provide estimates of the emissions for a far larger portion of the city, and ideally for the city as a whole.

Near ground sites are cheaper and easier to install and maintain than tall towers, which raise problems of accessibility. There are far more choices of location for the placing of instrumentation near ground than on tall towers, even within a city. The development of cheaper instruments could enable the deployment of networks with numerous sites and this is likely to require placement of at least some sites on near ground locations. If near ground sites can be used effectively they could be highly complementary to the developing GHG observation networks. Kort et al. (2013) evaluated (through Observing System Simulation Experiments, which is a common practice in the data assimilation community, as detailed by Masutani, 2010) different configurations of surface stations for monitoring emissions from Los Angeles, and concluded that robust monitoring of megacities requires multiple in-city surface sites (numbering at least eight stations for Los Angeles). McKain et al. (2012) employed near ground sites in Salt Lake City, an urban area that is relatively small and topographically confined. They concluded that surface stations could be used to detect changes in emission at the monthly scale, but not to derive estimates of the absolute emissions because of the inability of current models to simulate small-scale atmospheric processes.

In this study, we focus our attention on the megacity of London, UK. Quasi-continuous measurements of CO_2, CH_4 and CO were made during 2012 at four sites in the London area (two inner city sites, one suburban site and one rural site outside the urban area) using sensors located at 10–15 m a.g.l. We assess the ability of a km-gridscale transport model driven by a km-gridscale emissions inventory to simulate these CO_2 and CH_4 measurements. The aim is to understand whether such measurement sites are ultimately suitable for use in a flux inversion scheme based on the km-gridscale model. This study investigates the weight of different sources of misfits between observed and simulated GHG mole fractions (henceforth "model–data misfits"). We attempt to separate the signature of these different sources of misfits to

ACPD
15, 33003–33048, 2015

isolate and exploit the signature of the errors in the estimates of the urban emissions. We focus on the following sources of model–data misfits:

1. The differences of representativity in terms of spatial scale: near ground sites are sensitive to very local emissions, i.e., at scales smaller than those represented by the model.

2. Uncertainties in the meteorological conditions: the model cannot perfectly simulate the wind speed and direction and the mixing layer height above the city.

3. Uncertainties relating to both the conditions at the model domain boundaries and to fluxes outside of the London area: a large part of the variability of the concentrations in the London area is due to remote fluxes and conditions.

4. In the case of CO_2, uncertainties related to remote or near-field natural fluxes: the mixing between the natural and anthropogenic signal in the CO_2 measurements requires accurate information on the natural fluxes or a method for separating them to avoid projecting errors in the natural fluxes into errors in the anthropogenic emissions.

We introduce the measurement sites and model configuration in Sect. 2. In Sect. 3 we first consider issues of spatial representativity (Sect. 3.1) and then the ability of the model to simulate the diurnal cycle of mixing layer height, CO, CO_2 and CH_4 (Sect 3.2). In Sect. 3.3 we compare the model's simulated winds to measurements at two surface meteorological stations. In Sect. 3.4 we examine the day-to-day variations of measured and modelled CO_2 and CH_4. We attempt to remove the influence of the remote fluxes and conditions by considering gradients in CO_2 and CH_4 across the city in Sect. 3.5, and then take into account the wind direction when selecting the gradients (Sect. 3.6). Finally, we evaluate the modelled fossil-fuel CO_2 using a simple method to estimate the anthropogenic component of the observed CO_2 mole fractions based on the continuous CO observations (Sect. 3.7). A summary and discussion of the overall findings of the research is then given in Sect. 4.

ACPD
15, 33003–33048, 2015

2 Methodology

2.1 London emissions inventory for CO_2 and CH_4

As context for the location of the in situ measurements, and to provide an estimate of the emissions applied within the model, we utilise the United Kingdom National Atmospheric Emissions Inventory (NAEI, 2013). The NAEI provides annual gridded emission data for a wide range of atmospheric pollutants and GHGs with a sectorial distribution by the main types of emitting activities: agricultural soil losses, domestic (commercial, residential, institutional) combustion, energy production, industrial combustion, industrial production processes, offshore own gas combustion, road transport, other transport, solvent use, waste treatment and disposal and (for CH_4 only) agricultural emissions due to livestock and natural emissions. Major CO_2 and CH_4 point sources (comprising large power and combustion plants) are also listed and localised individually. The methodology applied to derive these gridded maps is described in Bush et al. (2010).

The most up-to-date published emissions estimates available from NAEI at the time of this study were for 2009. The CO_2 emissions for the region around London are shown at 2 km resolution (the resolution of simulated transport; see Sect. 2.4) in Fig. 1 along with the position of the measurement stations (Sect. 2.2). In the vicinity of London, nearly all the point sources of CO_2 are related to combustion processes with emissions from high stacks and through warm plumes. The 10 largest emitters in the domain defined by Fig. 1 are power stations, which represent nearly 27 % of the emissions in this domain.

2.2 GHG measurement site locations and characteristics

The four measurement sites were located in and around London to sample air masses passing over London at various levels of sensitivity to urban emissions (city centre, suburban and rural). Note that no formal quantitative network design was applied be-

ACPD
15, 33003–33048, 2015

forehand to select the optimal location of the stations for their ability to constrain the emissions of London. The station locations were rather chosen based on the configuration of the emissions given by the inventory maps and the availability of suitable locations for installation and maintenance of the instruments.

The site locations are shown in Fig. 1 and were operational between June and September 2012. The two urban sites of Hackney and Poplar were located in central London, 6 km apart from each other and to the north-east of the main area of emissions (Hackney at 51°33′31.45″, −0°3′25.44″; Poplar 51°30′35.67″, −0°1′11.33″). The suburban site was located in Teddington (51°25′13.63″, −0°20′21.15″), 15 km south-west of the city centre. The location of this site was chosen a priori to allow the analysis of the gradient due to the city emissions when the wind blows from the south-west, which is usually the case. The fourth site was located in Detling, Kent (51°18′28.44″, 0°34′57.36″), in a rural area ≈ 50 km from the inner city and was selected to help to detect the influence of remote fluxes on the GHG mole fractions over the city.

The measurement stations at Hackney and Poplar were located on the rooftop of a college and a primary education school, respectively. The inlets for each of these sensors were placed approximately 10 m above street level and approximately 2 m above the rooftop level. The NAEI emissions map (Fig. 1) shows substantial CO_2 sources west of the Poplar and Hackney sites, relating to the city centre.

The site in Teddington was located on top of a building approximately 15 m from ground level and 17 km south-west of Central London. Teddington is referred to in this study as a suburban site, due to its location in a residential area beside Bushy Park. Bushy Park represents a large area of vegetation cover surrounding the site to the east, south and west with residential and commercial land use located to the north.

The site in Detling was located on the top of a 10 m mast at an established air quality measurement site in a pasture field approximately 2 km from the nearest major roads.

ACPD
15, 33003–33048, 2015

2.3 GHG measurements

Continuous measurements of CO, CO_2, CH_4 and water vapour were taken between 1 June and 30 September 2012 for the Hackney, Poplar and Teddington sites and 5 July to 30 September 2012 at Detling. Each site was instrumented with a G2401 Picarro CRDS that logged data every 5 s and sent data files each hour to a remote server.

All sensors across the network were manually calibrated on an approximately two-weekly basis using the same gas standards, ensuring the consistency of the measurements from different sites. The sensors were calibrated for linearity, repeatability of measurements (for zero and span gases, i.e., respectively with concentrations zero and close to ambient air) and drift in the field and in the laboratory prior to deployment. The synthetic standards including the zero and span gases were prepared by National Physical Laboratory (NPL) as described in Brewer et al. (2014) with mole fractions close to those of atmospheric ambient air (379 ± 0.95 parts per million (ppm) CO_2 and 1800 ± 5 parts per billion (ppb) CH_4; uncertainties being expressed as 1-sigma standard deviations, SD). A higher than ambient concentration of CO was used (9.71 ± 0.015 ppm), because of the unavailability of low CO standards at the time of the experiment, leading to high uncertainties in CO measurements in ambient air.

The design of the experiment should have included independent measurements using a target gas of flask samples as recommended by the World Meteorological Organisation (WMO) Expert group to quantify possible biases. However, the fact that we were using similar analysers at the four stations, operated with the same protocols and calibrated with a single reference scale, reduced the risk of systematic biases between the sites. The high 1-sigma uncertainties in the molar fraction of gases used for the calibration result in biases that are common to all sites for the measurement period since the same gas cylinders were used for all stations throughout the period (the calibration error due to uncertainty in the calibration gas depends on the ambient concentration, but this dependence is such that the resulting variability of the calibration error is clearly negligible compared with the variability of the concentrations in time or between sites).

ACPD
15, 33003–33048, 2015

For this reason, the calibration biases mostly cancel out when analysing gradients of ambient molar fractions between the different sites of the network (this may not hold for higher molar fractions). This bias precludes, however, the use of this network in combination with other stations that have a different calibration standard.

In addition, there was a random measurement error of SD 0.26 ppm for CO_2, 8 ppb for CH_4 and 15 ppb for CO. This error budget includes drifts and variability in read-outs when measuring zero and span gases, as well as the applied correction for water vapour on the CO_2 and CH_4 channels. Measurements of CO_2 and CH_4 were taken from the dry channel to which an automatic correction had been applied for variability due to water vapour (Rella et al., 2013). The uncertainty associated with applying the water vapour correction was estimated to be 0.021 ppm for CO_2 and 0.1 ppb for CH_4. No water correction was applied for CO. Expressed as a percentage of the mean measured concentration throughout the measurement period, the total measurement uncertainties (including bias and random error) are 0.30, 0.67 and 21.3 % for CO_2, CH_4 and CO, respectively.

Data were calibrated using the standard gas cylinder values, and provided as 15 min averages by NPL. Calibration episodes were removed from the final dataset. The Teddington sensor was inactive between 6 and 12 July due to sample pump failure and there were a small number of missing days at Detling (due to power outage) and at Poplar (for unknown reasons). There was little missing data at the Hackney site. The 15 min data from the measurement sites were aggregated by averaging into hourly time intervals for comparison with the hourly output from the model. If fewer than four 15 min data points were available for any given hour (usually as a result of periodic data scan by the Picarro analyser or return to functionality after a calibration event or instrument downtime), the corresponding hourly average was removed from the analysis to maintain consistency between the model and data hourly averaged values.

ACPD
15, 33003–33048, 2015

2.4 Simulation of the atmospheric transport of CO_2 and CH_4

To model the transport of CO_2 and CH_4 mole fractions over London, we used a "South of England" configuration of the mesoscale atmospheric transport model CHIMERE (Schmidt et al., 2001). This model has already been used for CO_2 transport and flux inversion at regional to city-scale (Aulagnier et al., 2010; Broquet et al., 2011; Bréon et al., 2015). The domain over which CHIMERE was applied in this study (area ~ 49.9–53.2° N, −6.4–2.4° E) covers the whole South of England to minimise the impact of defining model boundary conditions using coarser model simulations close to the measurement sites. Additionally, the boundaries were traced as much as possible in the seas, in particular the western boundary from which the dominant winds flow over England. However, the northern boundary crosses England and the south-eastern part of the domain overlaps a small part of Northern France.

The model has a regular grid with 2 km horizontal resolution and 20 vertical levels from the ground up to 500 hPa (with ~ 20–25 m thicknesses close to the ground). CHIMERE is driven by atmospheric mass fluxes from the operational analyses of the European Centre for Medium-Range Weather Forecasts (ECMWF) at 3 h and ~ 15 km horizontal resolution (which are interpolated linearly on the CHIMERE grid and every hour). In this study, these mass fluxes were processed before their use in CHIMERE to account for the increased roughness in cities and in particular in London: the surface wind speed was decreased proportionally to the fraction of urban area in each model grid cell (the decreases in horizontal wind speed are balanced by an increase of the vertical component of the wind). However, the current configuration does not account for the urban heat island either in the ECMWF product or in the processing of this product before its use by CHIMERE.

The simulations were initialised on 15 April 2012. For the CO_2 simulations, the initial mole fractions and the open boundary conditions (at the lateral and top boundaries of the model) were imposed using simulated CO_2 from the Monitoring the Atmospheric Composition and Climate Interim Implementation (MACC-II, 2012) forecasts at

ACPD
15, 33003–33048, 2015

~ 80 km resolution globally (Agustí-Panareda et al., 2014). The MACC-II forecast was initiated on 1 January 2012 with online net ecosystem exchange (NEE) from the CTESSEL model (see the description below of the estimate of natural fluxes used for the CHIMERE simulations) and prescribed fossil fuel CO_2 emissions and air–sea fluxes, and is not constrained by CO_2 observations. For the CH_4 with CHIMERE, the initial and boundary conditions were imposed homogeneously in space and time to be equal to 1.87 ppm, according to the typical mole fractions measured at the Mace Head atmospheric measurement station in 2012 (NOAA., 2013). The top boundary conditions were set to a smaller value: 1.67 ppm.

Anthropogenic emissions of CO_2 and CH_4 were prescribed to CHIMERE within its domain using the NAEI emission inventory described in Sect. 2.1. Three dimensional hourly emissions for CO_2 and CH_4 were interpolated from this inventory on the 2 km horizontal resolution model grid. The derivation of the emission for the UK based on the NAEI inventory included injection heights for major point sources and temporal profiles (see below the details on the definition of injection heights and temporal profiles). The CO_2 emissions for the small part of France appearing in the domain were derived from the Emission Database for Global Atmospheric Research (EDGAR, 2014) at 0.1° horizontal resolution for the year 2008. Injection heights and temporal variations were ignored for this part of France.

The definition of injection heights can have a large impact when modelling the transport of CO_2 mole fractions from combustion point sources (Bieser et al., 2011). Many parameters underlying the effective injection heights for each source are not available (e.g., the stack heights, the flow rate and the temperature in the stacks). Furthermore, this study focuses on data during summer, and, as indicated later, during the afternoon when the troposphere is well-mixed so that the impact of the injection heights is minimum. Therefore, we derived approximate values for these heights as a function of the sectors associated with the point sources only, and based on the typical estimates by sector for nitrogen oxide gases (NO_x), CO and SO_2 (and for neutral atmospheric temperature conditions) from Pregger and Friedrich (2009). The resulting injection heights

ACPD
15, 33003–33048, 2015

for the emissions listed as point sources by the NAEI inventory (other emissions were prescribed at ground level) ranged from the second vertical CHIMERE level (~ 25 to 55 m above ground level; m a.g.l.) for the smallest industrial and commercial combustion plants to the 8 vertical CHIMERE level (~ 390 to 490 m a.g.l.) for the power stations. All CH_4 emissions sources were prescribed at ground level.

The variations of CO_2 and CH_4 in time are strongly driven by those of the emissions at the hourly to the seasonal scale (Reis et al., 2009). In the modelling framework of this study, temporal profiles were derived for the three sectors of CO_2 emissions with the largest variations in time: road transport, power generation in large combustion plants, and residential and commercial combustion. They were based on Reis et al. (2009) using data from 2004 to 2008. These sectorial profiles were applied homogeneously in space for the whole South of England. For road transport, the profiles were based on the combination of monthly variations for a typical year, daily variations for a typical week and hourly variations for each day of the week (with two maxima during week days and one maximum for Saturdays and Sundays) derived from statistical data about the traffic flows in the UK. For the power generation and residential and commercial combustion, monthly variations only were considered based on the consumption for typical years. We do not attempt to derive temporal profiles for the CH_4 emissions, which instead remain constant in time.

Natural fluxes of CO_2 were taken from the 15 km resolution NEE product from ECMWF (Boussetta et al., 2013), which is calculated online by the CTESSEL land surface model coupled with the ECMWF numerical weather prediction model.

Ocean fluxes for both gases within the domain were ignored because they are considered negligible at the timescales considered in this study. At the spatial and temporal scales considered in this study, the loss of CH_4 through chemical reactions is also negligible and was thus ignored here.

The model tracks the transport of the total CO_2, but also of its different components separately: CO_2 from the boundaries (BC-CO_2), from the NEE (BIO-CO_2) and from

ACPD
15, 33003–33048, 2015

fossil-fuel emissions (FF-CO_2). The model does not track CO mole fractions; however, the CO measurements are used to evaluate the FF-CO_2 in Sect. 3.7.

The 15 km resolution of the ECMWF analyses, used as meteorological forcing for CHIMERE, yields relatively uniform wind speed and direction at the city scale. The interpolation of this product on the 2 km CHIMERE grid is compared with the observations from surface meteorological sites located in and around London in Sect. 3.3.

2.5 Meteorological measurements

An important contribution to model–data misfits arises from errors in the representation of meteorological conditions; particularly wind speed and direction, and mixing later height. To evaluate the meteorological forcing of CHIMERE, hourly observations of wind speed and direction were collected from the UK Met Office Integrated Data Archive System (MIDAS) (UK Meteorological Office, 2012). The measured wind data were obtained for 10 m a.g.l. at Heathrow Airport, London (51°28′43.32″, −0°26′56.54″) and East Malling, Kent (51°17′15.36″, 0°26′54.24″). East Malling is located 6 km from the Detling site and Heathrow is located 7 km from the Teddington site and 18 km from the Hackney and Poplar sites. The locations of the meteorological sites are shown in Fig. 1.

Observed winds at East Malling were compared with winds from ECMWF (interpolated on the CHIMERE grid) at the lowest level (0–25 m) and at the corresponding location of the CHIMERE grid. Observed winds at Heathrow were compared with the next CHIMERE level up (25–50 m), because the urban roughness correction had been applied to the lowest level. This avoids strong biases in the model–data comparison that would arise because the urban roughness correction was necessarily applied in a homogenous way for the corresponding model grid cell, while, in reality the sites were not located within the urban canopy.

Hourly mean mixing height measurements were collected from a Doppler lidar that was located on the grounds of a school in North Kensington (51°31′13.97″, −0°12′50.85″) as part of the Clearflo project (Bohnenstengel et al., 2014). The lim-

ACPD
15, 33003–33048, 2015

ited sampling rate of the lidar was accounted for using a spectral correction method described in Barlow et al. (2014) and Hogan et al. (2009). Mixing heights were calculated based on a threshold value of the vertical velocity variance, perturbed between 0.080 and 0.121 $m^2 s^{-1}$. Mean, median, 5 and 95th percentile values were calculated for each hour based on these perturbations, and account for both measurement and method uncertainties (Barlow et al., 2014; Bohnenstengel et al., 2014). Based on the 5th and 95th percentile data averaged across all data for each hour, estimated measurement and method uncertainty was between 53 and 299 m throughout the daily cycle, with the highest uncertainties usually overnight. These measurement uncertainties are small when compared with the amplitude of the observed diurnal cycle shown in Fig. 3a. Lidar data were available for the period between 23 July 2012 and 17 August 2012 and were compared with the modelled boundary layer height (diagnosed in the ECMWF forecast using a critical value of 0.25 for the bulk Richardson number) at North Kensington during the same period.

3 Results and discussion

The data used for all statistical diagnostics of the model–data misfits in this section (including the wind roses and mean diurnal cycles in Figs. 2 and 3) are for the period 5 July to 30 September 2012 since data were available at all GHG sites during this period. The analyses of model–data misfits in GHG mole fractions utilise the hourly average of the 15 min aggregate measurements (Sect. 2.3) and the analyses of meteorological measurements relate to hourly data for the same period. However, some of the figures with timeseries of the GHG concentrations display the GHG available data in June 2012.

ACPD
15, 33003–33048, 2015

3.1 First insights on the influence of local sources on urban GHG measurements

We first consider the representativity of the CO_2 and CO at the urban sites by analysing them as a function of wind speed and direction. Figure 2 shows wind roses at Hackney and Poplar for measured CO and CO_2, and modelled CO_2, alongside aerial images of the site locations. To reduce the influence of boundary layer variation on the measured and modelled mole fractions, and to anticipate the data selection on which the study will focus, we include measured and modelled data for the afternoon period only (see Sect. 3.2).

At Hackney there is a clear increase in measured CO and CO_2 mole fractions during periods of south-easterly wind (Fig. 2a and b). A busy roundabout is located approximately 10 m to the south-east of the Hackney site with an A-road running from north to south to the east of the sensor location (Fig. 2d). There is no increase for south-easterly winds when analysing modelled CO_2 (Fig. 2c) suggesting that the observed increase in the measurements could be related to the roundabout whose specific influence cannot be represented at the 2 km resolution in the model.

At Poplar, the measured CO and CO_2 is more uniform than at Hackney (Fig. 2e and f). It is still higher in the east but there is no clear signature of the busy roads to the north and south of the site (Fig. 2h). The modelled CO_2 at Poplar (Fig. 2h) is very similar to that of Hackney (Fig. 2c), which can be explained by the proximity between the two corresponding model grid cells (Fig. 1). This supports the earlier assumption that the high mole fractions obtained at Hackney for south-easterly winds are related to a local source. These analyses also raise a more general assumption that while the model simulates the signature of emissions at a relatively large scale (due to handling emissions and transport at a 2 km resolution and with significant numerical diffusion) in the area of these 2 sites, there are likely to be local-scale unresolved emissions strongly influencing observed CO_2 at both of the urban sites.

ACPD
15, 33003–33048, 2015

At both sites the observed CH_4 wind roses are very similar, showing increased mole fractions towards the east of the site (data not presented); however, mole fractions are greater in magnitude at Poplar than Hackney. Similarly to CO_2, the model simulates lower CH_4 mole fractions than observed with a similar distribution at both sites. The stronger similarity between the wind roses at the two sites when considering CH_4 measurements than when considering CO_2 measurements could be explained by the absence of strong CH_4 local sources in the vicinity of the measurement sites.

Despite this potential influence of local sources that are unresolved by the transport model, we attempt, in the following, to understand and decompose the large misfits between the model and the measurements illustrated in Fig. 2. The objective is to analyse whether one can identify the signature of errors in the emissions at scales larger than 2 km × 2 km which should give insights on the potential for applying atmospheric inversion.

3.2 CO_2, CH_4 and mixing layer mean diurnal cycles

The mean observed and modelled diurnal cycles of the CO, CO_2 and CH_4 mole fractions at the four GHG measurement sites and the mixing layer height at North Kensington (see Sect. 2.5) are presented in Fig. 3. The amplitude of the mean diurnal cycle in mixing layer height (Fig. 3a) is approximately 1500 m, typical of summer convective conditions in an urban area (Barlow et al., 2014).

Observed CO_2 mole fractions at all sites follow a typical mean diurnal cycle (Fig. 3) with maximum mole fractions in the early morning (approx. 05:00, UTC being used hereafter) and minimum mole fractions during the afternoon (approx. 15:00), which can be related to the typical variation in mixing height (Fig. 3a), and in vegetation CO_2 exchanges (with photosynthesis and a CO_2 sink during daytime but CO_2 emissions during night-time) during a daily cycle. The early morning peak in CO_2 mole fractions occurs on average an hour later at the inner city sites (06:00) compared with the rural and suburban sites (05:00) as shown in Fig. 3c and e. This may be due to the signature of working-week urban emissions with a peak in traffic around 06:00 to 09:00. This is

ACPD
15, 33003–33048, 2015

supported by large observed CO mole fractions at the urban sites with substantial early morning and evening peaks (Fig. 3b). The peak in CH_4 measured mole fractions occurs at around 06:00 at all sites (Fig. 3d and e).

We now consider the ability of the model to simulate the diurnal cycle of CO_2 and CH_4 mole fractions. At all sites there is an underestimation of observed CO_2 and CH_4 mole fraction during the afternoon hours (12:00 to 17:00). This underestimation is between 1 and 5 % of the observation mean and is consistently larger than the confidence intervals for the averaging (associated with the limited time sampling) indicated throughout Fig. 3. The underestimation continues throughout the diurnal cycle at Detling and Teddington (Fig. 3c and d); however, at the urban sites (Fig. 3e and f), the night-time (00:00 to 05:00) CO_2 and CH_4 mole fractions are considerably larger in the model than in the observations. This overestimation is outside of the given confidence intervals for the averaging (associated with the limited time sampling) for most of the overnight period and leads to excessively strong diurnal variations at the urban sites, with the exception of CH_4 at Poplar (Fig. 3f).

Mixing layer height is underestimated in the model at North Kensington by approximately 13 % of the equivalent lidar measurement during the night and 33 % during the afternoon (Fig. 3a). This can explain the overestimation of mole fractions at the urban sites during night-time but this suggests that there would be further underestimation of CO_2 and CH_4 mole fractions during the afternoon if the modelled boundary layer height was closer to the measured one. This underestimation should thus be driven by other sources of misfits which will be explored in later sections.

Accurate modelling of the boundary layer height in meteorological models is an ongoing concern, particularly in urban areas (Gerbig et al., 2008; Lac et al., 2013) and description of nocturnal stratification is weak in atmospheric transport models (Geels et al., 2007). During the night there can be a considerable urban heat island in London as shown for North Kensington and rural Chilbolton by Bohnenstengel et al. (2014). The model used in our study does not currently have an urban land-surface scheme capable of reproducing the urban heat island effects on atmospheric transport (Sect. 2.4). This

ACPD
15, 33003–33048, 2015

may explain the different sign of the model–data misfits during night-time between the urban sites and the other sites. We thus restrict the remaining analyses in this paper to the period between 12:00 and 17:00, wherein we can expect the boundary layer to be well developed, to have a stable height and to exert minimum influence on the variations in gas mole fractions (Geels et al., 2007; Göckede et al., 2010).

3.3 Comparison of modelled and measured winds

This section focuses on the horizontal wind, which is a critical driver of day to day variations in GHG mole fractions. We aim to validate the model wind forcing through comparison with meteorological sites described in Sect. 2.5. The analyses of measured and modelled wind are restricted to between 12:00 and 17:00 because all further GHG analyses are focused on this afternoon period (Sect. 3.2).

At East Malling, on average, the model underestimates windspeed by 0.50 $m\,s^{-1}$ (12 % of the observation mean) and wind direction by 6.90° (defining positive angles clockwise hereafter). The root mean square (RMS) of model–data misfits is 1.10 $m\,s^{-1}$ for wind speed and 26° for wind direction. At Heathrow Airport, there is an average bias of 0.37 $m\,s^{-1}$ (7 % of observation mean) and 5° for wind speed and direction respectively (RMS misfits = 1.27 $m\,s^{-1}$ and 2.24° for wind speed and direction respectively). Some of this misfit may arise from the necessity of taking the 25–50 m average wind data from the model compared with the 10 m height measurements at the Heathrow meteorological station.

Lac et al. (2013) employed the Meso-NH meteorological model at 2 km horizontal resolution with an urban surface scheme that models specific energy fluxes between urban areas and the atmosphere. Their modelled meteorology was compared with meteorological stations in the Paris region. They showed a typical bias of 0.8 $m\,s^{-1}$ for wind speed and 20° for wind direction, which is larger than the agreement obtained here with the ECMWF winds driving CHIMERE at a native resolution of 15 km. Nehrkorn et al. (2013) found a wind speed bias of between −1 and 2.5 $m\,s^{-1}$ and RMS of between 1 and 4 $m\,s^{-1}$ using the WRF model at 1.33 km resolution over Salt Lake City, US, with

ACPD
15, 33003–33048, 2015

an urban land surface scheme. Therefore, the choice of a 15 km wind field to force the CHIMERE transport model over London may not be optimal but does not seem to raise typical wind errors larger than when using a state of the art meteorological model at kilometric resolution.

3.4 Daily CO_2 and CH_4 mole fractions during the mid-afternoon

The average CO_2 and CH_4 mole fractions for the afternoon of each day throughout the analysis period are presented in Figs. 4 and 5. Some data have been excluded from these analyses; we ignore hereafter, at a given site, any hour during which either modelled or measured data were not available. We have also excluded data from 29 August and 23 to 24 September since the model simulated very large GHG peaks on these days which do not occur in the data. Data from June have been excluded from statistical analysis to maintain comparability with Detling at which data were not available during this month.

According to both the measurements and the model, there is a clear difference in both the mean value and variability of CO_2 and CH_4 mole fractions between the urban sites Hackney and Poplar (Figs. 4b and c, 5b and c) compared with the rural and suburban Detling and Teddington sites (Figs. 4a and d, 5a and d). Both the modelled and observed CO_2 and CH_4 mole fractions increased in magnitude between Detling and Teddington and the inner city (Hackney and Poplar) sites as would be expected as a result of their relative distance to the main area of anthropogenic emission in the centre of London (Fig. 1) and due to the location of Teddington (Detling) to the south-west (south-east) of the London area while the dominant wind directions are from the west.

Statistical comparisons between modelled and measured hourly CO_2 and CH_4 mole fractions are given in Table 1. While the magnitude of the SD of the misfits is similar to that of the bias for CO_2, it is far larger than the bias for CH_4. The negative bias in modelled CO_2 mole fractions during the afternoon period (Sect. 3.2) is highest at the Hackney site (Table 1). The RMS of model–data misfits is likewise highest at Hackney

ACPD
15, 33003–33048, 2015

(12 ppm) but similar at the other three sites (8 to 9 ppm, Table 1). The model consistently underestimates CH_4 by more than 10 ppb at all sites, with the highest underestimation at Poplar (Table 1). Higher RMS of model–data misfits are found at Poplar and Hackney (48 and 55 ppb) than at Teddington and Detling (32 and 33 ppb) (Table 1).

The model–data misfits are substantially larger than measurement error for both CO_2 and CH_4 (Table 1) so we can exclude measurement error as a key source of the misfit. The misfit should mainly be associated with representation errors (Sect. 3.1), transport errors (Sect. 3.3) errors in the domain boundary-conditions and in the prescribed fluxes within the domain and outside the London area, or with errors in the inventory of the emissions prescribed in the London area.

The variations in modelled hourly afternoon CO_2 mainly follow the signal transported from the MACC-II boundary conditions (BC-CO_2 in Fig. 4) even at urban sites. The correlation between the hourly model signal and the hourly BC-CO_2 is very high at all sites (between 0.75 and 0.85, depending on the site) implying a strong dependence on the BC-CO_2. The CH_4 time series, which uses a constant value at the boundaries, cannot show such a dependence (Fig. 5). Model–data correlations are significantly higher for hourly CH_4 than for hourly CO_2 (between 0.02 and 0.13 for CO_2 and between 0.42 and 0.58 for CH_4, depending on the sites). However, the amplitude of the variations of CH_4 is so different between the model and the measurements that it yields the very large model–data misfits given in Table 1. This suggests that the actual CH_4 conditions on the boundaries of the modelling domain could have a strong influence on the variations of measured CH_4, as for CO_2, but we miss it through the use of constant boundary conditions in the model.

3.5 CO_2 and CH_4 gradients between pairs of sites

The findings of substantial misfits between observed and modelled GHGs at the four sites, the strong influence of boundary conditions on the modelled CO_2, and the potential issue raised by using a constant boundary condition for the CH_4 simulations, leads us to analyse the CO_2 or CH_4 gradient between the urban sites and the rural or

ACPD
15, 33003–33048, 2015

suburban sites. Because of this computation, the rural and suburban sites are called hereafter "reference sites". This gradient calculation should enable us to reduce the influence both of the CO_2 or CH_4 boundary conditions, and of the fluxes that are outside the London area but within the model domain (Bréon et al., 2015). This assumes that such an influence has a large spatial and temporal scale and is therefore similar for different sites within the London area. This analysis requires data at both the urban and the reference sites for a given hour and thus adds a new criterion to the data time selection already described and applied in Sect. 3.4. The gradients are henceforth described as follows; Hackney and Detling (HAC–DET), Hackney and Teddington (HAC–TED), Poplar and Detling (POP–DET) and Poplar and Teddington (POP–TED).

Figure 6 presents the daily afternoon mean gradients of measured and modelled CO_2 and CH_4 mole fractions (ΔCO_2 and ΔCH_4) alongside the daily afternoon mean gradient of modelled FF-CO_2 and BIO-CO_2 components (ΔFF-CO_2 and ΔBIO-CO_2) from the model simulation. It is clear from Fig. 6 that the modelled ΔCO_2 closely tracks modelled ΔFF-CO_2, while the ΔBIO-CO_2 is relatively small. This fit between ΔCO_2 and ΔFF-CO_2 implicitly indicates that the influence of the boundary conditions on these gradients is also relatively small, particularly when Teddington is used as the reference site. This strongly supports the assumption that the signature of boundary conditions and fluxes outside the London area operates on a large spatial and temporal scale and is therefore similar between different sites within the London area, even though this cannot be directly verified from the measurements. We thus expect that both the modelled and measured gradients between the urban and the reference sites bear a clear signature of the anthropogenic emissions from the London area.

The largest hourly ΔCO_2 are observed on the HAC–DET gradient with a mean (±SD) of 8.2 ± 5.3 ppm. The hourly POP–DET gradients have a mean (±SD) of 5.6 ± 4.6 ppm. These are larger than the gradients observed between a tall tower in central London and a rural location by Rigby et al. (2008).

The bias, SD and consequently RMS of the model–data misfits between modelled and measured gradients of both CO_2 and CH_4 (Table 2) are much reduced compared

ACPD
15, 33003–33048, 2015

with the same metrics at individual urban sites (Table 1). The RMS of the model–data misfits is roughly halved for ΔCO_2 compared with site CO_2. There is also a small improvement in correlation between observed and modelled ΔCO_2 compared with correlation between observed and modelled CO_2 at individual urban sites (from between 0.02 and 0.13 to between 0.20 and 0.35), but model–data correlations for ΔCH_4 are reduced compared with those for CH_4 at the individual urban sites (from between 0.42 and 0.58 to between 0.20 and 0.30).

The measurements at each site are affected by a constant calibration bias (see Sect. 2.3), therefore the decrease in model–data biases after the gradient computation partially comes from the cancellation of this systematic error. However, this systematic error is much smaller than the difference between the model–data biases when considering the analysis of mole fractions at individual sites and those when considering gradients between these sites. Furthermore, assuming that the random component of the measurement errors is uncorrelated between different sites (which should be the case in principle), this random measurement error should be larger for gradients than at individual sites. Therefore, the main driver of the strong decrease of model–data misfits when analysing gradients instead of mole fractions at individual sites should be the strong reduction of the large scale errors from the boundary conditions and remote fluxes.

Assuming that the random component of the measurement errors is uncorrelated between different sites, the standard deviation of the gradient measurement error should be the product of the standard deviation of the measurement error at individual sites by a factor $\sqrt{2}$. Therefore, the gradient measurement error should remain much smaller than the gradient model–data misfits, and the gradient model–data misfits should mainly be related to model (transport and representation) errors and errors in the estimate of fluxes in the London area.

ACPD
15, 33003–33048, 2015

3.6 CO_2 and CH_4 gradients with wind direction filtering

Figure 6 shows that the fit between the modelled ΔCO_2 and $\Delta FF\text{-}CO_2$ is better for gradients to Teddington than to Detling. This is likely to be because Teddington is far closer to London's centre than Detling (Fig. 1), and because Teddington is more frequently upwind of the city than Detling. The signature of fluxes outside the London area can be assumed to be more homogeneous along the wind direction than over the whole London area. It should therefore be more efficient to decrease the signature of the fluxes outside London by considering gradients between two sites along the wind direction than by considering the gradients between any two sites in the London area for any wind condition (Bréon et al., 2015). We therefore expect the gradients to Teddington to be representative of the London urban emissions more often than gradients to Detling. Gradients calculated without considering the wind direction, particularly gradients to Detling, are thus expected to retain a significant influence of the boundary conditions and fluxes outside the London area and can reach negative values even though they should bear the signature of the London emissions (Fig. 6).

Therefore, to reduce the influence of remote fluxes and increase the signature of the London urban emission when analysing the gradients, we next select gradients for periods wherein the corresponding reference site is upwind of the corresponding urban site. In practice, we select the gradient between an urban site and the reference site when the wind direction measured at Heathrow (if the reference site is Teddington) or East Malling (if the reference site is Detling) is within a $\pm 20^{\circ}$ range around the direction from the reference site to the urban site. The selected gradients correspond to 18 % of the afternoon HAC–TED available afternoon gradients and 16 % of the POP–TED available afternoon gradients. There are only 17 hourly gradients to Detling (3 % of all available afternoon gradients to Detling) recorded wherein Detling was positioned upwind of the urban sites. Because of this low number of selected observations, gradients to Detling are ignored in the remainder of the analyses.

ACPD
15, 33003–33048, 2015

The statistics of the model–data misfits for gradients to Teddington when this site is upwind of the urban sites are presented in Table 2. Filtering for wind direction reduced the negative bias and the RMS of misfits for ΔCO_2 HAC–TED gradients, but slightly increased the RMS of misfits and increased the positive bias on the ΔCO_2 POP–TED gradient relative to analysis without wind filtering. The resulting SD of the misfits has values that correspond to the typical observation and model transport errors identified by other inverse modelling studies, e.g., Bréon et al. (2015) diagnose a 3 ppm standard deviation of the observation error for gradients in the Paris area. However, the bias in ΔCO_2 for both HAC–TED and POP–TED after wind filtering is within the range of 1 to 2 ppm which remains relatively high. There is underestimation at Hackney and overestimation at Poplar. Regarding ΔCH_4, all the statistics of the model data misfits after wind filtering are improved substantially, resulting in the RMS misfits being roughly halved when comparing the statistics with and without wind filtering.

To increase the number of selected gradients and thus the robustness of the statistics, we next conduct a test wherein the constraint on the wind direction is relaxed to ±40° around the direction from the suburban to the urban site. The resulting bias and RMS of model–data misfits for ΔCO_2 are very similar for HAC–TED with a range of ±20° around the direction from the suburban to the urban site (with bias of −1.8 ppm and RMS of the misfits of 3.4 ppm). However, the ±40° wind direction improves the statistics at Poplar (with bias of 0.9 ppm and RMS of model–data misfits of 3.1 ppm). While this option yields better results in general, it diverges from the principle of monitoring the gradients of concentration along the transport direction only.

Since local sources have been identified as a potential major source of model data misfits, a further analysis of the gradients when the wind direction is within a ±20° range around the direction from the suburban to the urban site is conducted by selecting only gradients to Teddington (Detling) when both the hourly mean wind speed measured at Heathrow (East Malling) and modelled at Teddington (Detling) are above 3 $m\,s^{-1}$. Such a threshold is assumed to decrease the influence of local sources on the variations of the GHG mole fractions (Bréon et al., 2015). However, the sensitivity to this selection is

ACPD
15, 33003–33048, 2015

relatively weak and only slightly improves the results for ΔCH_4 and for ΔCO_2 for HAC–TED and slightly increases the misfits for ΔCO_2 for POP–TED, while further decreasing the number of observations and thus the robustness of the statistics.

3.7 Estimation of the fossil fuel component of the CO_2 mole fractions

While the signature of the fossil fuel emissions dominates in the modelled gradient between urban and suburban CO_2 (Sect. 3.5), the contribution of the natural fluxes is not systematically null. The residual misfits when comparing measured and modelled gradients can also question the validity of the assumption that the signature of the natural fluxes is not significant compared with that of the fossil fuel emissions in the measured gradient.

In this section we thus attempt to improve the focus on the signature of the urban emissions by deriving a CO_2 fossil fuel component from both the modelled and the measured gradients. While the model directly provides the ΔFF-CO_2 values, we use an empirical method based on the continuous CO measurements to extract an observation based estimate of ΔFF-CO_2 between the measurement sites, since CO and CO_2 are co-emitted when fossil fuels are burnt. We focus the analysis on HAC–TED and POP–TED when Teddington is located upwind of the urban sites (with a $\pm 20^{\circ}$ margin for the selection of the corresponding wind direction), given that such a choice increases the consistency between the model and the data (Sect. 3.6).

The ratio of CO to FF-CO_2 (henceforth R) varies depending on the different type of sources (e.g., traffic, industry) whose relative influence at the measurement sites can vary in time due to changing transport conditions. However, we assume that these relative influences on HAC–TED and POP–TED gradients are constant in time during the afternoon when Teddington is upwind of the urban sites. We also assume that CO acts as a conservative tracer and does not interact with the surrounding environment during its transport throughout the London urban area (Gamnitzer et al., 2006). Consequently, we assume that *R* resulting from the combination of all sources is constant for gradients between two given sites. Using CO gradients and this ratio, one can derive the

ACPD
15, 33003–33048, 2015

observation based ΔFF-CO_2 using the following equation (Eq. 1):

$$FFCO_2 = \frac{CO_{urb} - CO_{suburb}}{R}, \quad FFCO_2 = \frac{CO_{urb} - CO_{suburb}}{R} \tag{1}$$

where CO_{urb} is the observed CO mole fractions at the urban site and CO_{suburb} is the observed CO mole fractions at the suburban Teddington site.

We can assume a traffic-dominated value of R during summer as we can anticipate lower energy consumption due to natural gas burning in the surrounding area (Vogel et al., 2010). Examination of the diurnal cycle of CO at the urban sites revealed the typical traffic-based variability of increased mole fractions in the early morning and late afternoon and larger CO mole fractions during the day than overnight (Sect. 3.2, Fig. 3b). A value of 0.011 is given to R based on the literature that has evaluated traffic dominated values of R in urban areas using the ^{14}C isotope (Wunch et al., 2009; Vogel et al., 2010; Newman et al., 2013). We further assume that the errors in observation based ΔFF-CO_2 are smaller than the model or actual ΔFF-CO_2 variations.

Modelled ΔFF-CO_2 is on average slightly larger than observation-based ΔFF-CO_2 on the HAC–TED gradient (mean observed ΔFF-CO_2 of 6.2 ± 2.3 ppm and modelled ΔFF-CO_2 of 5.8 ± 3.8 ppm). On the POP–TED gradient, observation-based ΔFF-CO_2 is considerably lower than the modelled ΔFF-CO_2 (mean observation-based ΔFF-CO_2 of 3.5 ± 1.0 ppm and modelled ΔFF-CO_2 of 6.3 ± 2.9 ppm). Statistical comparisons between modelled and observation-based ΔFF-CO_2 mole fractions are given in Table 3. Compared with ΔCO_2 (Table 2), we see a very strong reduction in bias and RMS on the HAC–TED gradient when considering the fossil fuel component only. However, the bias is significantly increased in misfits on the POP–TED gradients when comparing results for ΔFF-CO_2 to those for ΔCO_2.

ACPD
15, 33003–33048, 2015

4 Concluding remarks

In this study we compared observed CO_2 and CH_4 mole fractions from four near ground measurement sites in and around London to the simulations from a mesoscale transport model driven by temporally and spatially varying emissions estimates. We aimed to understand whether these near ground sites would be amenable to the atmospheric inversion of the London city-scale emissions using such an atmospheric transport model. The measurements and model simulation applied to the period June–September 2012. Given the initial diagnostic of very large model data misfits at the different measurement sites, this study attempted to remove or characterise the influence of some of the underlying sources of uncertainty and to isolate, in both the model and the measurements, the signal that corresponds to the London anthropogenic emissions which would be targeted by the inversion.

Focusing the analysis on afternoon data limits the impact of the model's inability to correctly predict the transitions of the mixing layer depth in morning and evening. This problem is acknowledged in other greenhouse gas transport studies (Denning et al., 1999; Geels et al., 2007; Lac et al., 2013). It is possible that this is exacerbated here because of London's urban heat island, which is significant overnight (Barlow et al., 2014; Bohnenstengel et al., 2014), while the model's meteorological forcing does not include a true urban parameterization.

Focusing the analysis on gradients between the urban sites and the reference sites, especially when selecting them for periods when the suburban reference site is upwind of the urban sites, strongly reduced the impact of errors from the boundary conditions and fluxes outside of the London area in the modelling configuration. Since these boundary conditions and remote fluxes were shown to strongly drive the time variations of the mole fractions in the London area, this focus yielded a relatively low time-varying component of the model–data misfits. According to the model, this gradient computation also allowed isolation of the signature of the London anthropogenic emissions from that of the natural fluxes in the area. The very good fit between the modelled fos-

ACPD
15, 33003–33048, 2015

sil fuel CO_2 gradient between Hackney and Teddington (when Teddington is upwind of Hackney) and the CO measurement based estimate of this gradient (even though this estimate relies on crude assumptions regarding the correlation between CO and fossil fuel CO_2) could further support the assumption that the urban to suburban along-wind gradient bears a very strong signature of the London emissions that is consistent between the model and the measurements.

However, there are large biases between the modelled fossil fuel CO_2 gradient between Poplar and Teddington (when Teddington is upwind of Poplar) and the CO measurement-based estimate of this gradient, and between the modelled and measured CO_2 gradients between the urban and reference sites (filtering or not by the wind direction so that the reference site is upwind of the urban site). These biases could be related to biases in the estimate of anthropogenic emissions in the model. However, there is a clear difference between the measured gradients from Hackney to Teddington and those from Poplar to Teddington, while the model predicts similar gradients when considering either urban site. This results in model–data biases with opposed signs depending on the urban site considered. This implies that such biases are more likely to be related to local sources that cannot be represented in the 2 km resolution model than to biases in the city-scale estimate of the anthropogenic emissions in the model. The influence of the local traffic source, identified southeast of the Hackney site in Sect. 3.1, should be removed from the analysis of gradients to Teddington when Teddington located upwind i.e., west of Hackney. However, other smaller sources are likely to occur nearby to the urban sites.

For CH_4 there is greater similarity between observations or between the model simulations at the two urban sites. This suggests that there are no CH_4 local sources near to these sites, which is reasonable because the major CH_4 sources in urban environments are mainly related to a limited number of specific waste processing sites or to points of leakage in the gas distribution network. This, and the poorer representation of the boundary conditions for CH_4 in the model, can explain why the CH_4 misfits were

ACPD
15, 33003–33048, 2015

reduced more successfully than the CO_2 misfits when switching from the analysis of data at individual sites to the analysis of gradients.

The errors in the meteorological forcing could also participate to such biases. The biases between this forcing and measured wind in terms of biases in wind speed ($0.37\,m\,s^{-1}$ i.e., 7 % of observation mean) and in terms of biases in wind direction (5°) were smaller than reported by other studies (Lac et al., 2013), but could be highly problematic in a urban environment with highly heterogeneous sources in the vicinity of the measurement sites (Bréon et al., 2015). The meteorological forcing was also shown to underestimate the mixing layer depth during the afternoon.

Furthermore, we assessed measurement error as a potential source of model–data misfits throughout the analyses. The practical constraints for this short measurement campaign did not allow us to design it in such a way that the measurements can be compared with each other or with other measurements within 0.1 ppm, as recommended by WMO for the Northern Hemisphere (WMO, 2012). The random measurement error at individual sites was smaller than the model–data misfits by an order of magnitude so was considered to be negligible. However, the systematic measurement error is large enough not to be neglected in the raw misfits, even though it does not dominate. By definition, the unknown offset in our network vanishes when inter-site gradients are considered, but only because a unique calibration cylinder was used for all sites and for the whole measurement period, which is not a robust solution for larger and longer-lasting local networks. This unknown offset hampers any comparison with other measurement sites in the UK or other places in the world that can therefore not be assimilated in the same inverse modelling system as our London city measurements.

As a result, the amplitude of the model–data misfit in the gradients is often as large as that of the measured gradients, in particular for CH_4, which is not optimistic regarding the ability to adjust the estimate of the London urban emissions. For CH_4, the specific point sources are generally monitored individually (Yver Kwok et al., 2015) since CH_4 emissions are neither diffuse nor significant enough in the urban environment to be monitored using a city scale atmospheric inversion approach.

ACPD
15, 33003–33048, 2015

For CO_2, as discussed above, these misfits mainly consist of biases that do not occur on large spatial scales. This raises strong challenges for the inversion of the CO_2 emissions using a 2 km resolution transport model. The location of the urban measurement sites close to the ground, where the sensitivity to local sources is very high, may be responsible for such an issue. Therefore, this study strongly questions the ability to exploit a GHG network with near ground urban measurement sites alongside a state of the art atmospheric inversion system with atmospheric transport models at kilometric horizontal resolution. Complementing such models using high resolution dispersion models would be necessary both for studying the representativity of potential location of such near ground urban measurement sites, and ultimately to conduct atmospheric inversions using these sites.

Acknowledgements. This work was funded and supported by Astrium Services SAS. The authors would like to thank Brian Sweeney of the National Physical Laboratory for his efforts in keeping the measurement sites calibrated and well maintained. We would like to thank the Clearflo project members for provision of the lidar data from their summer IOP at North Kensington and thanks go to Christos Halios for help with interpreting the lidar data. Thanks also go to Davey Atkinson for help with figure preparation.

References

Agustí-Panareda, A., Massart, S., Chevallier, F., Boussetta, S., Balsamo, G., Beljaars, A., Ciais, P., Deutscher, N. M., Engelen, R., Jones, L., Kivi, R., Paris, J.-D., Peuch, V.-H., Sherlock, V., Vermeulen, A. T., Wennberg, P. O., and Wunch, D.: Forecasting global atmospheric CO_2, Atmos. Chem. Phys., 14, 11959–11983, doi:10.5194/acp-14-11959-2014, 2014.

Aulagnier, C., Rayner, P., Ciais, P., Vautard, R., Rivier, L., and Ramonet, M.: Is the recent build-up of atmospheric CO_2 over Europe reproduced by models – Part 2: an overview with the atmospheric mesoscale transport model CHIMERE, Tellus B, 62, 14–25, doi:10.1111/j.1600-0889.2009.00443.x, 2010.

ACPD
15, 33003–33048, 2015

Barlow, J. F., Halios, C. H., Lane, S. E., and Wood, C. R.: Observations of urban boundary layer structure during a strong urban heat island event, Environ. Fluid Mech., 15, 373–398, doi:10.1007/s10652-014-9335-6, 2014.

Bieser, J., Aulinge, A., Matthias, V., Quante, M., and van der Gon, H.: Vertical emission profiles for Europe based on plume rise calculations, Environ. Pollut., 159, 2935–2946, doi:10.1016/j.envpol.2011.04.030, 2011.

Bohnenstengel, S. I., Belcher, S. E., Aiken, A., Allan, J. D., Allen, G., Bacak, A., Bannan, T. J., Barlow, J. F., Beddows, D. C. S., Bloss, W. J., Booth, A. M., Chemel, C., Coceal, O., Di Marco, C. F., Dubey, M. K., Faloon, K. H., Fleming, Z. L., Furger, M., Gietl, J. K., Graves, R. R., Green, D. C., Grimmond, C. S. B., Halios, C. H., Hamilton, J. F., Harrison, R. M., Heal, M. R., Heard, D. E., Helfter, C., Herndon, S. C., Holmes, R. E., Hopkins, J. R., Jones, A. M., Kelly, F. J., Kotthaus, S., Langford, B., Lee, J. D., Leigh, R. J., Lewis, A. C., Lidster, R. T., Lopez-Hilfiker, F. D., McQuaid, J. B., Mohr, C., Monks, P. S., Nemitz, E., Ng, N. L., Percival, C. J., Prévôt, A. S. H., Ricketts, H. M. A., Sokhi, R., Stone, D., Thornton, J. A., Tremper, A. H., Valach, A. C., Visser, S., Whalley, L. K., Williams, L. R., Xu, L., Young, D. E., and Zotter, P.: Meteorology, air quality, and health in London: the ClearfLo project, B. Am. Meteorol. Soc., 96, 779–804, doi:10.1175/BAMS-D-12-00245.1, 2014.

Boussetta, S., Balsamo, G., Beljaars, A., Panareda, A.-A., Calvet, J.-C., Jacobs, C., van den Hurk, B., Viterbo, P., Lafont, S., Dutra, E., Jarlan, L., Balzarolo, M., Papale, D., and van der Werf, G.: Natural land carbon dioxide exchanges in the ECMWF integrated forecasting system: implementation and offline validation, J. Geophys. Res.-Atmos., 118, 5923–5946, doi:10.1002/jgrd.50488, 2013.

Bréon, F. M., Broquet, G., Puygrenier, V., Chevallier, F., Xueref-Remy, I., Ramonet, M., Dieudonné, E., Lopez, M., Schmidt, M., Perrussel, O., and Ciais, P.: An attempt at estimating Paris area CO_2 emissions from atmospheric concentration measurements, Atmos. Chem. Phys., 15, 1707–1724, doi:10.5194/acp-15-1707-2015, 2015.

Brewer, P. J., Brown, R. J. C., Miller, M. N., Miñarro, M. D., Murugan, A., Milton, M. J. T., and Rhoderick, G. C.: Preparation and validation of fully synthetic standard gas mixtures with atmospheric isotopic composition for global CO_2 and CH_4 monitoring, Anal. Chem., 86, 1887–1893, doi:10.1021/ac403982m, 2014.

Broquet, G., Chevallier, F., Rayner, P., Aulagnier, C., Pison, I., Ramonet, M., Schmidt, M., Vermeulen, A. T., and Ciais, P.: A European summertime CO_2 biogenic flux inversion at

ACPD
15, 33003–33048, 2015

mesoscale from continuous in situ mixing ratio measurements, J. Geophys. Res.-Atmos., 116, D23303, doi:10.1029/2011jd016202, 2011.
Bush, T., Tsagatakis, I., Passant, N., Griffin, A., and Pearson, B.: UK Emission Mapping Methodology 2007, Didcot, Oxfordshire, 52 pp., 2010.
Ciais, P., Paris, J. D., Marland, G., Peylin, P., Piao, S. L., Levin, I., Pregger, T., Scholz, Y., Friedrich, R., Rivier, L., Houwelling, S., Schulze, E. D., and Team, C. S.: The European carbon balance – Part 1: fossil fuel emissions, Glob. Change Biol., 16, 1395–1408, doi:10.1111/j.1365-2486.2009.02098.x, 2010a.
Ciais, P., Rayner, P., Chevallier, F., Bousquet, P., Logan, M., Peylin, P., and Ramonet, M.: Atmospheric inversions for estimating CO_2 fluxes: methods and perspectives, Climatic Change, 103, 69–92, doi:10.1007/s10584-010-9909-3, 2010b.
Denning, A. S., Holzer, M., Gurney, K. R., Heimann, M., Law, R. M., Rayner, P. J., Fung, I. Y., Fan, S.-M., Taguchi, S., Friedlingstein, P., Balkanski, Y., Taylor, J., Maiss, M., and Levin, I.: Three-dimensional transport and concentration of SF6, Tellus B, 51, 266–297, doi:10.1034/j.1600-0889.1999.00012.x, 1999.
Emissions Database for Global Atmospheric Research: available at: http://edgar.jrc.ec.europa.eu/index.php, last access: 13 January 2014.
Gamnitzer, U., Karstens, U., Kromer, B., Neubert, R. E. M., Meijer, H. A. J., Schroeder, H., and Levin, I.: Carbon monoxide: a quantitative tracer for fossil fuel CO_2?, J. Geophys. Res., 111, D22302, doi:10.1029/2005jd006966, 2006.
Geels, C., Gloor, M., Ciais, P., Bousquet, P., Peylin, P., Vermeulen, A. T., Dargaville, R., Aalto, T., Brandt, J., Christensen, J. H., Frohn, L. M., Haszpra, L., Karstens, U., Rödenbeck, C., Ramonet, M., Carboni, G., and Santaguida, R.: Comparing atmospheric transport models for future regional inversions over Europe – Part 1: mapping the atmospheric CO_2 signals, Atmos. Chem. Phys., 7, 3461–3479, doi:10.5194/acp-7-3461-2007, 2007.
Gerbig, C., Körner, S., and Lin, J. C.: Vertical mixing in atmospheric tracer transport models: error characterization and propagation, Atmos. Chem. Phys., 8, 591–602, doi:10.5194/acp-8-591-2008, 2008.
Göckede, M., Michalak, A. M., Vickers, D., Turner, D. P., and Law, B. E.: Atmospheric inverse modeling to constrain regional-scale CO_2 budgets at high spatial and temporal resolution, J. Geophys. Res.-Atmos., 115, D15113, doi:10.1029/2009JD012257, 2010.

ACPD
15, 33003–33048, 2015

Helfter, C., Famulari, D., Phillips, G. J., Barlow, J. F., Wood, C. R., Grimmond, C. S. B., and Nemitz, E.: Controls of carbon dioxide concentrations and fluxes above central London, Atmos. Chem. Phys., 11, 1913–1928, doi:10.5194/acp-11-1913-2011, 2011.

Hogan, R. J., Grant, A. L. M., Illingworth, A. J., Pearson, G. N., and O'Connor, E. J.: Vertical velocity variance and skewness in clear and cloud-topped boundary layers as revealed by Doppler lidar, Q. J. Roy. Meteor. Soc., 135, 635–643, doi:10.1002/qj.413, 2009.

Kort, E. A., Angevine, W. M., Duren, R., and Miller, C. E.: Surface observations for monitoring urban fossil fuel CO_2 emissions: minimum site location requirements for the Los Angeles megacity, J. Geophys. Res.-Atmos., 118, 1577–1584, doi:10.1002/jgrd.50135, 2013.

Lac, C., Donnelly, R. P., Masson, V., Pal, S., Riette, S., Donier, S., Queguiner, S., Tanguy, G., Ammoura, L., and Xueref-Remy, I.: CO_2 dispersion modelling over Paris region within the CO_2-MEGAPARIS project, Atmos. Chem. Phys., 13, 4941–4961, doi:10.5194/acp-13-4941-2013, 2013.

Levin, I., Hammer, S., Eichelmann, E., and Vogel, F. R.: Verification of greenhouse gas emission reductions: the prospect of atmospheric monitoring in polluted areas, Philos. T. R. Soc. A, 369, 1906–1924, doi:10.1098/rsta.2010.0249, 2011.

Lowry, D., Holmes, C. W., Rata, N. D., O'Brien, P., and Nisbet, E. G.: London methane emissions: use of diurnal changes in concentration and $\delta^{13}C$ to identify urban sources and verify inventories, J. Geophys. Res., 106, 7427, doi:10.1029/2000jd900601, 2001.

MACC-II: available at: www.copernicus-atmosphere.eu, last access: 1 September 2012.

Masutani, M., Schlatter, T. W., Errico, R. M., Stoffelen, A., Andersson, E., Lahoz, W., Woollen, J. S., Emmitt, G. D., Riishøjgaard, L.-P., and Lord, S. J.: Observing system simulation experiments, in: Data Assimilation: Making Sense of Observations, edited by: Lahoz, W. A., Khattatov, B., and Ménard, R., Springer, Berlin, 647–679, 2010.

McKain, K., Wofsy, S. C., Nehrkorn, T., Eluszkiewicz, J., Ehleringer, J. R., and Stephens, B. B.: Assessment of ground-based atmospheric observations for verification of greenhouse gas emissions from an urban region, Proc. Natl. Acad. Sci. USA, 109, 8423–8428, doi:10.1073/pnas.1116645109, 2012.

National Atmospheric Emissions Inventory: http://naei.defra.gov.uk/, access: 12/12/2013, 2013.

Nakagawa, F., Tsunogai, U., Komatsu, D. D., Yamada, K., Yoshida, N., Moriizumi, J., Nagamine, K., Iida, T., and Ikebe, Y.: Automobile exhaust as a source of C-13-

ACPD
15, 33003–33048, 2015

and D-enriched atmospheric methane in urban areas, Org. Geochem., 36, 727–738, doi:10.1016/j.orggeochem.2005.01.003, 2005.
Nehrkorn, T., Henderson, J., Leidner, M., Mountain, M., Eluszkiewicz, J., McKain, K., and Wofsy, S.: WRF Simulations of the Urban Circulation in the Salt Lake City Area for CO_2 Modeling, J. Appl. Meteorol. Clim., 52, 323–340, doi:10.1175/JAMC-D-12-061.1, 2013.
Newman, S., Jeong, S., Fischer, M. L., Xu, X., Haman, C. L., Lefer, B., Alvarez, S., Rappenglueck, B., Kort, E. A., Andrews, A. E., Peischl, J., Gurney, K. R., Miller, C. E., and Yung, Y. L.: Diurnal tracking of anthropogenic CO_2 emissions in the Los Angeles basin megacity during spring 2010, Atmos. Chem. Phys., 13, 4359–4372, doi:10.5194/acp-13-4359-2013, 2013.
NOAA Mace Head Atmospheric Station Data: available at: http://www.esrl.noaa.gov/gmd/dv/data/?site=MHD (last access: 23 January 2014), 2013.
Pregger, T. and Friedrich, R.: Effective pollutant emission heights for atmospheric transport modelling based on real-world information, Environ. Pollut., 157, 552–560, doi:10.1016/j.envpol.2008.09.027, 2009.
Reis, S., Lang, M., and Vieno, M.: Improving the temporal profiles of emission input data for high resolution atmospheric transport modeling - a case study for the UK, 18th Annual International Emission Inventory Conference, Baltimore, USA, 2009,
Rella, C. W., Chen, H., Andrews, A. E., Filges, A., Gerbig, C., Hatakka, J., Karion, A., Miles, N. L., Richardson, S. J., Steinbacher, M., Sweeney, C., Wastine, B., and Zellweger, C.: High accuracy measurements of dry mole fractions of carbon dioxide and methane in humid air, Atmos. Meas. Tech., 6, 837–860, doi:10.5194/amt-6-837-2013, 2013.
Rigby, M., Toumi, R., Fisher, R., Lowry, D., and Nisbet, E. G.: First continuous measurements of CO_2 mixing ratio in central London using a compact diffusion probe, Atmos. Environ., 42, 8943–8953, doi:10.1016/j.atmosenv.2008.06.040, 2008.
Schmidt, H., Derognat, C., Vautard, R., and Beekmann, M.: A comparison of simulated and observed ozone mixing ratios for the summer of 1998 in Western Europe, Atmos. Environ., 35, 6277–6297, doi:10.1016/s1352-2310(01)00451-4, 2001.
Townsend-Small, A., Tyler, S. C., Pataki, D. E., Xu, X., and Christensen, L. E.: Isotopic measurements of atmospheric methane in Los Angeles, California, USA: influence of "fugitive" fossil fuel emissions, J. Geophys. Res., 117, D07308, doi:10.1029/2011jd016826, 2012.

ACPD
15, 33003–33048, 2015

Met Office Integrated Data Archive System (MIDAS) Land and Marine Surface Stations Data (1853-current): available at http://badc.nerc.ac.uk/view/badc.nerc.ac.uk__ATOM__dataent_ukmo-midas (last access: 29 September 2013), 2012.

United Nations: World Population Prospects: 2011 Revision, available at: http://esa.un.org/unpd/wpp/publications/Files/WPP2012_HIGHLIGHTS.pdf (last access: 24 November 2015), 2012.

Vogel, F. R., Hammer, S., Steinhof, A., Kromer, B., and Levin, I.: Implication of weekly and diurnal 14C calibration on hourly estimates of CO-based fossil fuel CO_2 at a moderately polluted site in southwestern Germany, Tellus B, 62, 512–520, doi:10.1111/j.1600-0889.2010.00477.x, 2010.

GAW Report No. 206: available at: http://www.wmo.int/pages/prog/arep/gaw/documents/Final_GAW_206_web.pdf (last access: 9 August 2015), 2012.

Wunch, D., Wennberg, P. O., Toon, G. C., Keppel-Aleks, G., and Yavin, Y. G.: Emissions of greenhouse gases from a North American megacity, Geophys. Res. Lett., 36, L15810, doi:10.1029/2009gl039825, 2009.

Yver Kwok, C. E., Müller, D., Caldow, C., Lebègue, B., Mønster, J. G., Rella, C. W., Scheutz, C., Schmidt, M., Ramonet, M., Warneke, T., Broquet, G., and Ciais, P.: Methane emission estimates using chamber and tracer release experiments for a municipal waste water treatment plant, Atmos. Meas. Tech., 8, 2853–2867, doi:10.5194/amt-8-2853-2015, 2015.

ACPD
15, 33003–33048, 2015

Table 1. Summary of systematic and random errors of hourly measurements (see Sect. 2.3) and of the hourly model–data misfits using data between 12:00 and 17:00 during July to September 2012. Values are given for CO_2 (CH_4 in brackets) in parts per million (ppm) and parts per billion (ppb) for CH_4. SD denotes standard deviation; RMS denotes root mean square.

Error Type	Measurement error	Model–data misfits			
		Detling	Hackney	Poplar	Teddington
Bias	SD of bias: 1.0 (5.0)	−5.3 (−19.0)	−9.1 (−20.7)	−5.5 (−28.6)	−5.7 (−13.3)
SD	0.3 (8.0)	6.5 (27.4)	7.3 (43.2)	7.1 (46.9)	7.1 (29.3)
RMS	–	8.4 (33.3)	11.7 (47.9)	9.0 (54.9)	9.1 (32.2)

ACPD
15, 33003–33048, 2015

Table 2. Summary of systematic and random errors of hourly measured gradients (see Sect. 3.5, the standard deviation of the measurement error for gradients is computed as $\sqrt{2}$ times the value of Table 1, assuming null correlation of this error between different sites) and of the hourly gradient model–data misfits using data between 12:00 and 17:00 during July to September 2012. Values are given for ΔCO_2 (ΔCH_4 in brackets) in parts per million (ppm) and parts per billion (ppb) for CH_4. The two last columns present misfits for afternoon gradients to Teddington wherein Heathrow measured wind direction places Teddington upwind of each urban site (for angles between the wind direction and the direction between Teddington and a given urban site smaller than 20°, see Sect. 3.6). SD denotes standard deviation; RMS denotes root mean square.

	Gradient measurement error	All afternoon misfits				Teddington upwind misfits only	
		HAC–DET	POP–DET	HAC–TED	POP–TED	HAC–TED	POP–TED
Bias	SD of bias: 0.0 (0.0)	−3.8 (−2.6)	−0.2 (−9.7)	−2.9 (−7.1)	0.6 (−16.1)	−1.4 (−3.5)	1.7 (−10.8)
SD	0.4 (11.0)	5.1 (34.4)	4.4 (36.6)	4.2 (28.3)	3.6 (32.2)	2.9 (14.5)	3.4 (11.0)
RMS	–	6.3 (34.4)	5.1 (29.2)	4.4 (37.8)	3.6 (36.0)	3.2 (14.8)	3.7 (15.3)

ACPD
15, 33003–33048, 2015

Table 3. Statistics of the hourly difference between modelled ΔFF-CO_2 and observationally based ΔFF-CO_2 in parts per million (ppm) for HAC–TED and POP–TED during the afternoon periods (12:00 to 17:00) between July and September, when Heathrow measured wind direction places Teddington upwind of each urban site (for angles between the wind direction and the direction between Teddington and a given urban site smaller than 20°, see Sect. 3.6). RMS denotes root mean square.

Error Type	HAC–TED	POP–TED
Bias	−0.4	2.8
RMS	2.5	3.6

ACPD
15, 33003–33048, 2015

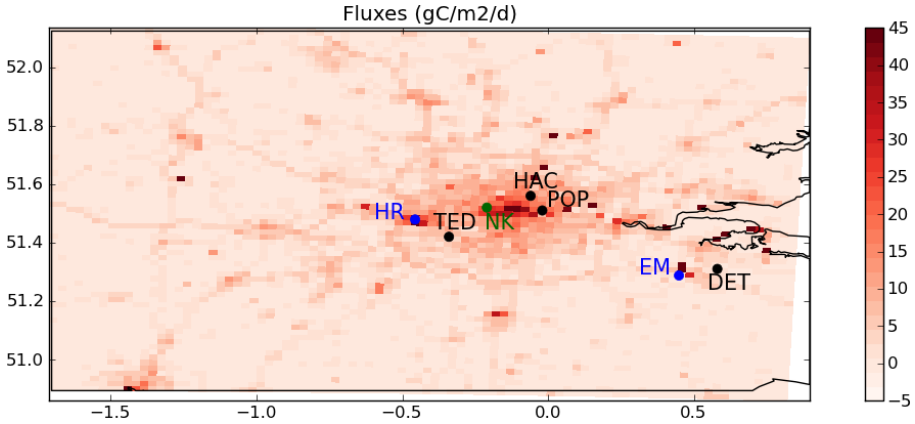

Figure 1. Map of the spatially derived (at 2 km resolution) CO_2 fossil fuel emissions inventories ($g\,C\,m^{-2}\,d^{-1}$) for the London section of the model domain, indicating the location of the four GHG measurement stations (black), the two meteorological sites (blue) and the North Kensington LIDAR site (green). Dark red corresponds to relatively high CO_2 values ($45\,g\,C\,m^{-2}\,d^{-1}$) and light pink to relatively low CO_2 values ($-5\,g\,C\,m^{-2}\,d^{-1}$).

ACPD
15, 33003–33048, 2015

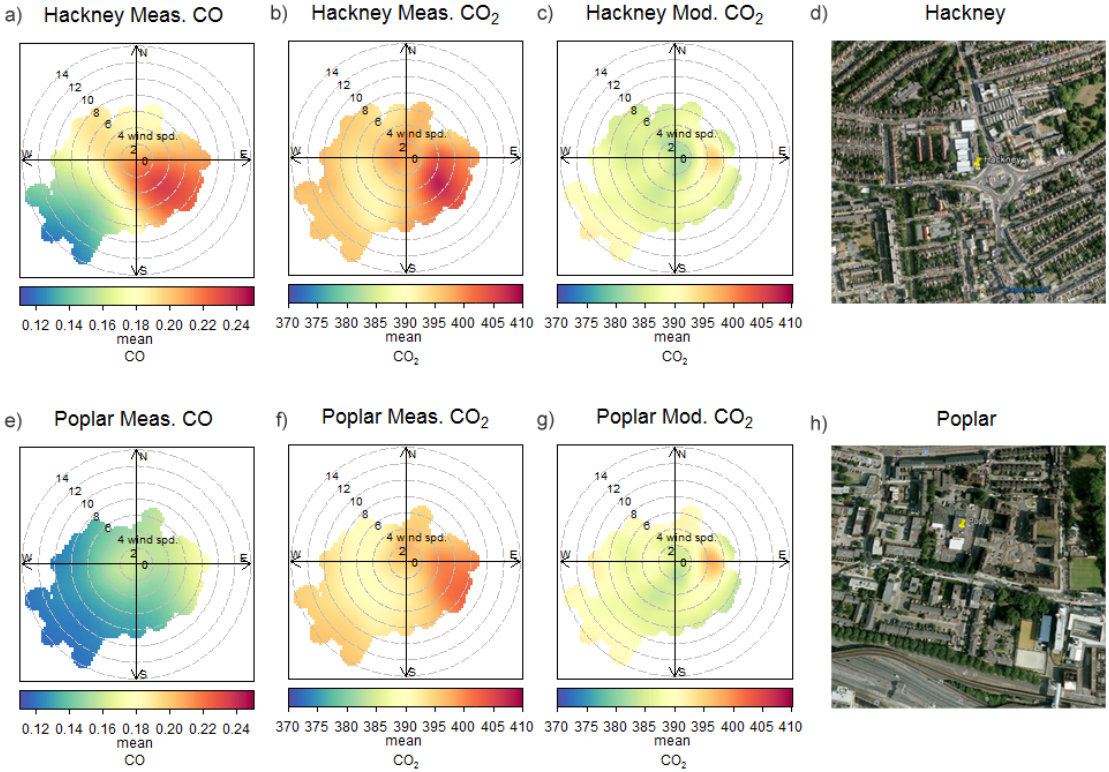

ACPD
15, 33003–33048, 2015

Monitoring and modelling of CO_2 and CH_4 in London

A. Boon et al.

Figure 2. Wind roses for each urban measurement site incorporating hourly data for wind speed, wind direction (Heathrow measured data) and CO_2 mole fraction between the hours 12:00 and 17:00 for **(a)** observed CO mole fractions at Hackney, **(b)** observed CO_2 mole fractions at Hackney, **(c)** modelled CO_2 mole fractions at Hackney, **(d)** a map (© 2012 Google-Imagery and Bluesky, the GeoInformation group) of the immediate vicinity of the Hackney site, **(e)** observed CO mole fractions at Poplar, **(f)** observed CO_2 mole fractions at Poplar, **(g)** modelled CO_2 mole fractions at Poplar and **(h)** a map (© 2012 Google-Imagery and Bluesky, the GeoInformation group) of the immediate vicinity of the Poplar site. The colours on the wind roses show the gas mole fraction (parts per million, ppm) with the radius corresponding to the magnitude of the windspeed ($m\,s^{-1}$) and the azimuthal angle to the wind direction (° N). Red corresponds to relatively high concentrations and blue to relatively low concentrations within the given scale of each gas (min = 0.11 parts per billion (ppb) and max = 0.25 ppb for CO, and min = 370 ppm, max = 410 ppm for CO_2).

ACPD
15, 33003–33048, 2015

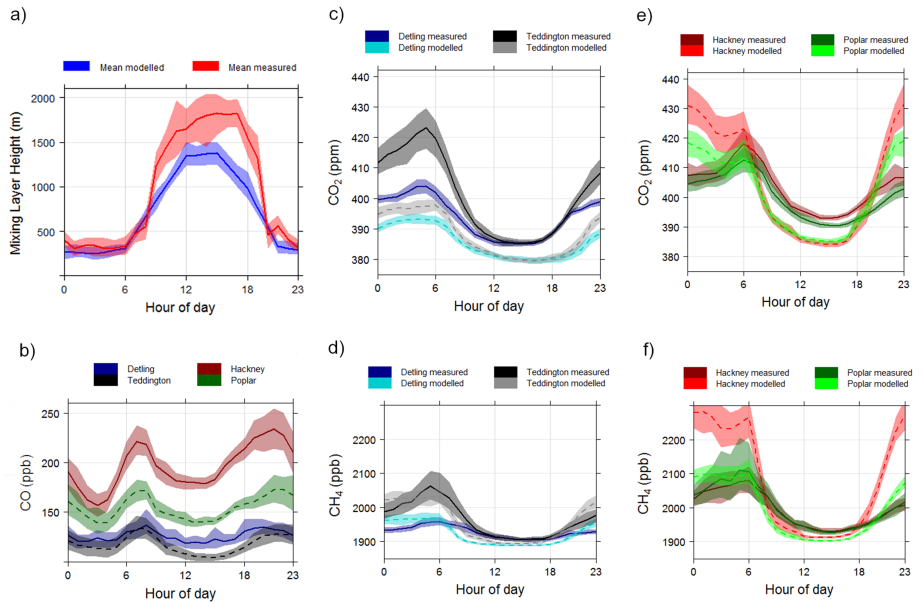

Figure 3. Mean diurnal cycles of **(a)** modelled (blue) and measured (red) boundary layer height and measured mean mixing layer height at North Kensington based on the spectral correction method described in Sect. 2.5, **(b)** measured CO mole fractions at the rural (Detling, blue), suburban (Teddington, black), and urban sites (Hackney, red and Poplar, green), **(c)** modelled (light shade) and measured (dark shade) CO_2 mole fractions at the rural (Detling, blue) and suburban (Teddington, black) sites, **(d)** modelled and measured (dark shade) CH_4 mole fractions at the rural (Detling, blue) and suburban (Teddington, black) sites **(d)** modelled (light shade) and measured (dark shade) CO_2 mole fractions at the urban (Hackney, red and Poplar, green) sites and **(f)** modelled and measured CH_4 mole fractions at the urban (Hackney, red and Poplar, green) sites. June data are excluded due to unavailability of data during this period at Detling. Shading represents an estimate of the 95 % confidence interval in the mean, related to the limitation of the sampling of the daily values at a given hour (based on the division of two times their temporal standard deviation by the square root of the number of values).

ACPD
15, 33003–33048, 2015

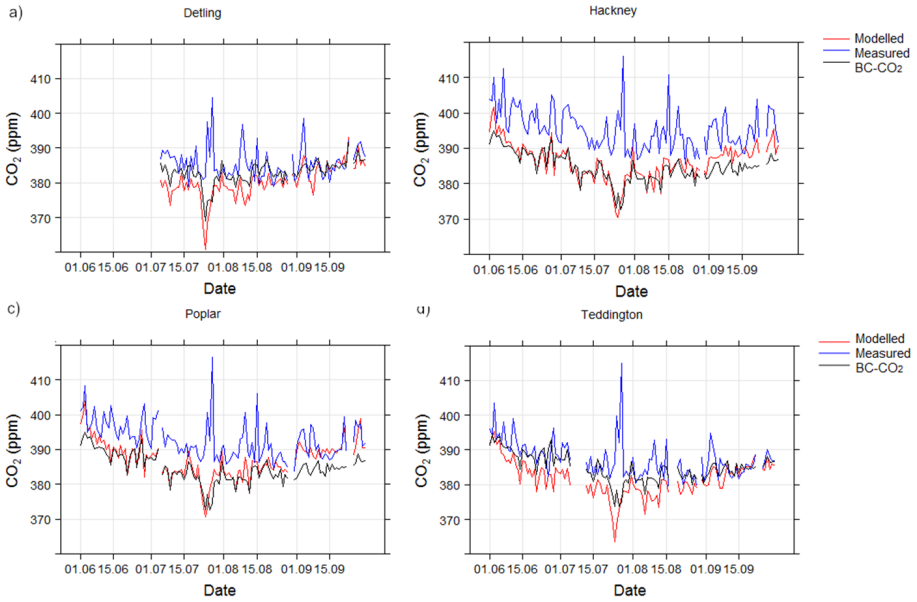

Figure 4. Time series of averages for the afternoon period (12:00 to 17:00) each day of measured CO_2 mole fractions (blue), modelled BC-CO_2 mole fractions from MACC-II (black) and modelled CO_2 mole fractions (red) at **(a)** Detling, **(b)** Hackney, **(c)** Poplar and **(d)** Teddington.

ACPD
15, 33003–33048, 2015

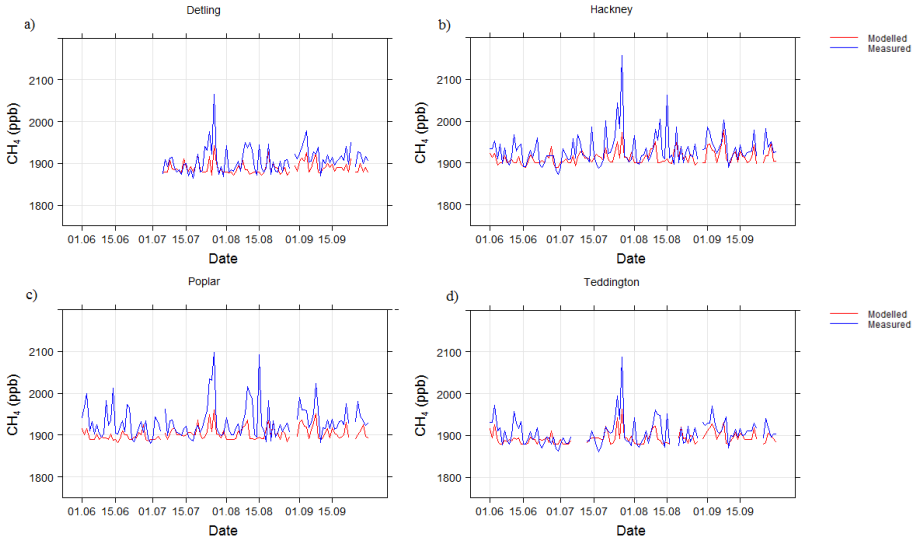

Figure 5. Time series of averages for the afternoon period (12:00 to 17:00) each day of measured CH_4 mole fractions (blue) and modelled CH_4 mole fractions (red) at **(a)** Detling, **(b)** Hackney, **(c)** Poplar and **(d)** Teddington.

ACPD
15, 33003–33048, 2015

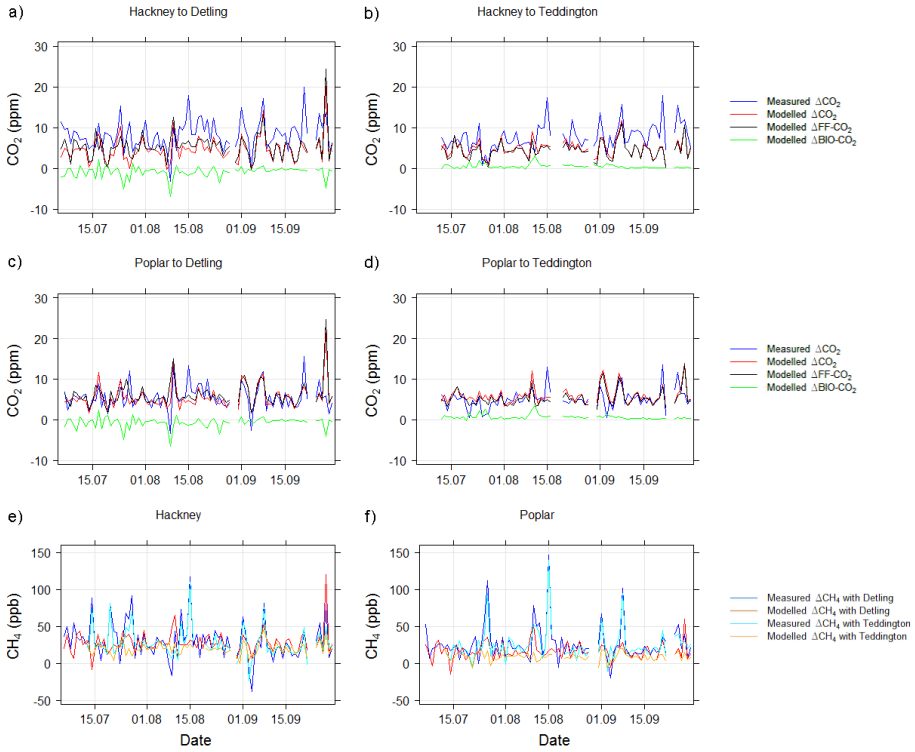

Figure 6. Time series of averages for the afternoon period (12:00 to 17:00) each day of measured ΔCO_2 (blue), modelled ΔCO_2 (red), modelled $\Delta FF\text{-}CO_2$ (black) and modelled $\Delta BIO\text{-}CO_2$ (green) between **(a)** Hackney and Detling, **(b)** Hackney and Teddington, **(c)** Poplar and Detling and **(d)** Poplar and Teddington. Time series of averages for the afternoon period (12:00 to 17:00) of measured (dark and light blue) or measured (red and orange) ΔCH_4 between **(e)** Hackney or **(f)** Poplar and Detling (dark blue and red) or Teddington (light blue or orange).

ACPD
15, 33003–33048, 2015